Cerebral Cortex June 2013;23:1362–1377
doi:10.1093/cercor/bhs120
Advance Access publication May 17, 2012

Two Distinct Ipsilateral Cortical Representations for Individuated Finger Movements

Jörn Diedrichsen[1], Tobias Wiestler[1] and John W. Krakauer[2,3]

[1]Institute of Cognitive Neuroscience, University College London, London, UK [2]Department of Neurology and [3]Department of Neuroscience, Johns Hopkins University, Baltimore, MD 21287, USA

Address correspondence to Jörn Diedrichsen, Institute of Cognitive Neuroscience, University College London, Alexandra House, 17 Queen Square, London WC1N 3AR, UK. Email: j.diedrichsen@ucl.ac.uk.

Movements of the upper limb are controlled mostly through the contralateral hemisphere. Although overall activity changes in the ipsilateral motor cortex have been reported, their functional significance remains unclear. Using human functional imaging, we analyzed neural finger representations by studying differences in fine-grained activation patterns for single isometric finger presses. We demonstrate that cortical motor areas encode ipsilateral movements in 2 fundamentally different ways. During unimanual ipsilateral finger presses, primary sensory and motor cortices show, underneath global suppression, finger-specific activity patterns that are nearly identical to those elicited by contralateral mirror-symmetric action. This component vanishes when both motor cortices are functionally engaged during bimanual actions. We suggest that the ipsilateral representation present during unimanual presses arises because otherwise functionally idle circuits are driven by input from the opposite hemisphere. A second type of representation becomes evident in caudal premotor and anterior parietal cortices during bimanual actions. In these regions, ipsilateral actions are represented as nonlinear modulation of activity patterns related to contralateral actions, an encoding scheme that may provide the neural substrate for coordinating bimanual movements. We conclude that ipsilateral cortical representations change their informational content and functional role, depending on the behavioral context.

Keywords: cortical representation, fMRI, motor cortex, multivoxel pattern analysis

Introduction

Finger movements appear to be (almost) exclusively controlled by cortical areas in the contralateral hemisphere—if control is defined as a direct connection to the spinal cord (Brinkman and Kuypers 1973; Soteropoulos et al. 2011). However, many cortical motor areas also show overall activity increases or decreases in relation to finger movements of the ipsilateral hand (Kim et al. 1994; Cramer et al. 1999; Hanakawa et al. 2005; Verstynen et al. 2005; Talelli, Waddingham et al. 2008; Horenstein et al. 2009). The functional role of these ipsilateral cortical changes remains unclear. An important first step in answering this question is to determine whether and how characteristics of ipsilateral actions are encoded in cortical circuits. This is based on the premise that a region that is involved in the control of movement, possibly through modulation of the other hemisphere, should contain neurons that are differentially active with respect to the relevant control variable. In other words, a region should contain a representation for the task control variable as a necessary (if not sufficient) condition for a region to play a functional role in control of this variable. For example, neurons in the hand area of the primary motor cortex show a differential tuning for different finger movements of the contralateral hand. Even though individual neurons respond to presses of multiple fingers (Schieber 2002; Acharya et al. 2008), and activation patches for individuated fingers overlap greatly (Indovina and Sanes 2001; Wiestler et al. 2011), the neuronal population as a whole encodes the exact action very precisely. In contrast, an area that shows exactly the same neuronal firing pattern regardless of the digit involved cannot play either a direct (cortico-spinal projections) or indirect (cortico-cortical modulation) role in "control" of individuated finger movements, but can at best have a supportive function, such as sustaining attention to the task or controlling postural muscles in a finger-invariant manner. Although the primary motor cortex appears to represent the movement direction of the ipsilateral arm (Donchin et al. 1998; Ganguly et al. 2009), there is currently no evidence for an analogous ipsilateral representation of individuated finger movements.

Using high-resolution functional magnetic resonance imaging (fMRI) and a statistical approach that tests for representation rather than average activation, we characterized how cortical motor areas represent ipsilateral isometric finger presses. If neurons are activated differentially for each finger, and if neuronal populations with similar properties are sufficiently clustered together, then we should be able to decode individual fingers from local fMRI activity patterns. Using this decoding approach, called multivoxel pattern analysis (MVPA, Kriegeskorte et al. 2006), we have recently found finger representations in the primary motor cortex and the cerebellum. It is noteworthy that this method, unlike a center-of-gravity (COG) analysis of individual fingers (Indovina and Sanes 2001), does not require any systematic somatotopy. Indeed, using this method, we were able to show finger representations in the inferior cerebellum, which lack any discernable somatotopic organization for individual fingers (Wiestler et al. 2011).

The experiments reported here show that there are 2 fundamentally different types of representation of ipsilateral fingers. During unimanual presses (Experiment 1), we find that the activity patterns elicited by each ipsilateral finger are highly correlated with those for the corresponding contralateral finger. Furthermore, these mirrored activation patterns disappear during bimanual finger presses (Experiment 2). Therefore, we conclude that ipsilateral representations during unimanual actions rely on the activation of the very same neuronal circuits that control the mirror-symmetric contralateral action. That is, if the 2 representations were at least partially independent, the region would have been able to represent both the ipsi- and contralateral actions simultaneously. A second type of ipsilateral representation becomes visible during bimanual actions. Here, both a premotor region and a parietal region encode unique

combinations of contra- and ipsilateral fingers. This type of representation is ideally suited to learning and controlling coordinated bimanual actions.

Materials and Methods

Participants

We tested 6 participants in Experiment 1 (unimanual left and right finger presses) and 7 in Experiment 2 (unimanual and bimanual presses). Four participants took part in both experiments, with at least 1 week separating the 2 experimental sessions. All participants were right-handed with an average laterality score (Oldfield 1971) of 0.88 (SD = 0.13), with 1 indicating the strongest right-hand preference and −1 the strongest left-hand preference. The average age was 25.9 years (SD = 5.1), and the sample included 6 men and 3 women. All experimental procedures were approved by the Ethics Committee of University College London.

Apparatus and Stimuli

Participants placed all 10 fingers on a keyboard, which was secured with a foam pillow on the participant's lap. The keyboard had 10 elongated keys, 20 mm wide, with a groove for each fingertip. A force transducer was mounted below each key and measured the force exerted by the finger. The force transducers (Honeywell FS series) had a dynamic range up to 16 N, with a repeatability of constant force measurements of <0.02 N. Signals from the force transducers were transmitted from the scanner room via a shielded cable. Filters in the scanner room wall prevented leakage of radiofrequency noise.

Participants executed isometric finger presses against the nonmovable keys. This setup allowed for very tight control of the behavior, while simultaneously monitoring for possible mirror movements. While isometric presses are technically not overt movements, they involve voluntary activation of specific muscles and produce sensory feedback commonly associated with full hand movements. Nonetheless, we refer to these actions as finger presses, to acknowledge the possibility that our results may not fully generalize to free finger movements.

Participants viewed a projection screen mounted behind the scanner bore via a mirror. The screen showed a central cross, on which participants were instructed to fixate during the entire experiment.

Image Acquisition

Data were acquired on a 3 T Siemens Trio system with a 32-channel head coil. Functional data comprised 8 runs of 126 volumes each, using a 2D echo-planar imaging sequence [repetition time (TR) = 2.72 s]. The first 3 volumes were discarded to allow magnetization to reach equilibrium. We acquired 32 slices in an interleaved sequence at a thickness of 2.15 mm (0.15 mm gap) and an in-plane resolution of 2.3×2.3 mm^2. The matrix size was 96×96. The slices covered the dorsal aspects of the cerebrum. The cerebellum and the inferior aspects of the occipital and temporal lobes were not covered. Field maps were obtained after the first functional run to correct for inhomogeneities in the main magnetic field (Hutton et al. 2002). We also acquired a single T1-weighted anatomical scan (3D magnetization-prepared rapid gradient echo sequence, 1 mm isotropic, $240 \times 256 \times 176$ mm field of view).

Procedure

To determine whether activity patterns observed during ipsilateral presses were finger-specific, we used a slow event-related design. On every trial (3 TRs = 8.16 s), participants made 5 paced isometric presses with the same finger. Each trial consisted of 6 short events, each 1.36 s long. The first event was the display of the instructional cue. The outline of the keyboard was presented, with each key shown in gray. The keys to be pressed were highlighted in green. After this event, the instructional cue was removed and instead of the fixation cross, the letter "P" was presented in white, signaling participants to make a short isometric force press with the instructed finger(s). When a finger press exceeded 2.3 N, a response was registered and the letter turned blue. If the participant accidentally pressed the wrong finger, the letter turned red. After 1.36 s, the letter turned white again, signaling the next finger press. After 5 finger presses, the trial ended. In most cases, the next trial began immediately afterwards with the display of the next instructional cue. In each run, we also randomly inserted 5 rest phases between trials, which lasted either 5 or 6 TRs.

Experiment 1 tested how the representation of ipsilateral finger movements relates to the representation of contralateral finger movements. Each of the 10 fingers was probed 3 times per run, resulting in 30 trials. The sequence of the fingers was fully randomized. Experiment 2 addressed the question of how representations of contra- and ipsilateral fingers interact during bimanual movements. To obtain enough data for each of the fingers, we studied only 3 of the fingers from each hand (digits 1, 3, and 5). Trials required either a single finger press on the left or right hand (unimanual) or a finger press on each hand (bimanual). All possible finger combinations were used, resulting in 6 unimanual and 9 bimanual trial types. Each trial type was repeated twice per run, yielding 30 trials per run.

First-Level Analysis

The functional data were analyzed using SPM8 (Friston et al. 1999) and custom-written Matlab code. First, we corrected for slice-acquisition timing by shifting the acquisition to align with the middle slice of each volume. We then corrected for head movements using a 6-parameter motion correction algorithm. This step also included correction of possible image distortions using the acquired fieldmap data (Andersson et al. 2001; Hutton et al. 2002). The realigned functional data were then coregistered to the anatomical scan, using the automatic algorithm in SPM. The coregistration was visually checked, and the affine parameters were adjusted by hand to improve the alignment in the region of the central sulcus, if necessary.

The preprocessed data were analyzed using a general linear model. To remove the influence of movement-related artifacts, we used a weighted least-squares approach (Diedrichsen and Shadmehr 2005). For each trial type (10 in Experiment 1 and 15 in Experiment 2), we defined 1 regressor per imaging run. The regressor was a boxcar function that started at the moment of the first finger press and lasted for 8 s. This function was convolved with the standard hemodynamic response function. Preliminary analyses showed that this function provided a very good fit to the movement-evoked response in the hand area of the primary motor cortex. The analysis resulted in 8 activation estimates (beta-images) for each trial type, 1 per run.

Surface-Based Analysis and Searchlight Approach

From the anatomical images, we obtained a surface reconstruction using the software Freesurfer (Dale et al. 1999), which estimates the outer boundary of the gray matter (pial surface) and the white–gray matter boundary (white surface). The surfaces were aligned via spherical registration to the Freesurfer average atlas (fsaverage, Fischl et al. 1999). Individual data were then projected onto the group map via the individual surface. Correction for multiple tests was performed on the surface using Gaussian field theory (Worsley et al. 1996).

To detect finger-specific representations anywhere in the cortex, we used a surface-based searchlight approach (Fig. 1; Oosterhof et al. 2011). We defined a circular region on the cortical surface and selected all voxels that lay, even partly, between the pial and white surfaces. For Experiment 1, we chose the radius such that 80 voxels were included. In Experiment 2, we required higher sensitivity to detect the relatively weak encoding for bimanual actions and therefore included 160 voxels. This resulted in an average searchlight radius of 6.9 or 9.8 mm, respectively. In comparison to standard volume-based searchlights (Kriegeskorte et al. 2006), a surface-based searchlight minimizes the bleeding of information from one region to the other across a sulcus and therefore allows for regionally specific inferences (Chen et al. 2011; Oosterhof et al. 2011). The activation estimates (beta-images) from the first-level analysis of the selected voxels were

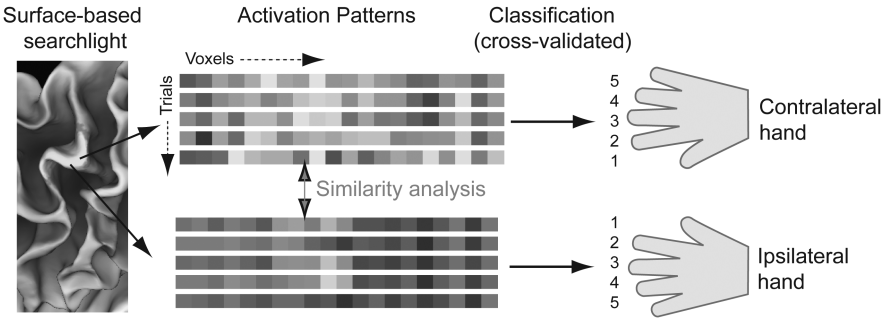

Figure 1. Multivariate analysis methods. On the reconstructed cortical surface, a circular area (searchlight) was selected. The activation values for all corresponding voxels (activation patterns) were extracted for all trials. A cross-validated classification approach was used for each hand separately to determine whether activation patterns contained information about the finger pressed. In areas with information about both contra- and ipsilateral fingers, we used a similarity analysis (Fig. 3) to determine the relationship between representation of contra- and ipsilateral fingers.

then submitted to a classification analysis (discussed subsequently), and the resulting classification accuracy was assigned to the center of the sphere. By moving this "searchlight" continuously over the cortical surface, we constructed a map describing how well the local voxel pattern represented the action of the contra- or ipsilateral finger.

Classification

If a region represents individuated finger movements, then local activity patterns should differ systematically for presses of different fingers. To test for such finger-specific activity patterns, we used a classification approach. A linear multiclass classifier was trained on data from 7 of the 8 imaging runs and then tested by classifying the finger presses on the 8th run (Pereira et al. 2009). By retraining and classifying over all possible test- and training-sets, we determined the average cross-validated accuracy for each set of voxels. The size of the classification accuracy can be taken as a measure of how strongly the activity patterns in this patch of cortex are modulated in a consistent finger-specific fashion.

As an input to the classifier, we used the activation estimates (beta-images) from the first-level analysis for P voxels. The classifier assumes that each pattern y_i ($Px1$ vector) comes from a multivariate normal distribution, with a condition-specific mean μ_c ($Px1$ vector) and a common PxP voxel-covariance matrix Σ. The conditions c relate here to the 5 fingers of a hand (unimanual classifier, Experiment 1) or to the 9 unique bimanual combinations (bimanual classifier, Experiment 2). The maximum-likelihood estimates for μ_c and Σ were derived from the training data. Because we had more voxels than trials, Σ was ill-conditioned, so we regularized the covariance estimate by adding a small constant (1% of the mean of the diagonal elements) to the diagonal (Pereira et al. 2009). We classified the pattern vectors y from the remaining run by calculating the discriminant function for each class c:

$$g_c(y) = \mu_c^{\mathrm{T}}\Sigma^{-1}y - \frac{1}{2}\mu_c^{\mathrm{T}}\Sigma^{-1}\mu_c \qquad (1)$$

This term is (up to a constant) the log-likelihood that the pattern y belongs to class c. The pattern was assigned to the class with the highest likelihood.

For Experiment 1 (unimanual presses only), we used 1 classifier to distinguish between the 5 fingers of the left hand and 1 classifier to distinguish between the 5 fingers of the right hand. Each classifier had a guessing baseline of 20%. For Experiment 2 (unimanual + bimanual presses), we used 3 separate classifiers, 1 for each unimanual condition and 1 for the bimanual condition. For the bimanual condition, we trained the classifier to distinguish between the 9 different trial types arising from the different finger combinations. That is, the classifier treated all categories independently, even though some combinations may have shared a finger. This ensured that the classifier could detect any form of bimanual encoding without any prior assumptions about the structure of the representation. For example, the classifier did not assume that patterns containing the same contralateral or ipsilateral finger were more similar to each other than patterns that did not.

From the predicted category, we could then calculate the classification accuracy for the ipsi- and contralateral fingers independently. For example, if the true action involved pressing both middle fingers, and the pattern was classified as involving contralateral middle and ipsilateral index finger press, then the contralateral finger would have been classified correctly and the ipsilateral finger incorrectly. Guessing baseline for all classification decisions in Experiment 2 was therefore 33%. For group analysis, the classification accuracies were transformed to z-scores, assuming a binomial distribution of the number of correct guesses. We then tested these z-scores against zero (guessing level) across participants.

Regions of Interests (ROIs)

To study the characteristics of the digit representations, we used both an anatomical and functional ROI approach. We defined the anatomical ROIs based on the probabilistic cytoarchitectonic maps aligned to the average Freesurfer surface (Fischl et al. 2008). The ROI for M1 comprised all of Brodmann area 4 (both rostral and caudal), and the ROI for S1 contained Brodmann areas 3a, 3b, 1, and 2. Brodmann area 6 was split into a lateral aspect [premotor cortex (PM)] and a medial aspect [supplementary motor area (SMA)/preSMA]. The superior parietal lobule (SPL) ROI included Brodmann area 7 (7A, 7P, and 7M) and medial intraparietal sulcus (IPS) (Scheperjans et al. 2008). The surface-based ROIs were projected into the volume using the individual surfaces. All voxels that touched one of the selected nodes on the white or pial surface were included in the ROI. To minimize the mixing of functional imaging signals across sulci, we excluded all voxels assigned to multiple ROIs from further analysis (e.g. voxels in the middle of the central sulcus). For some analyses, we combined M1 and PM to a precentral ROI and S1 and SPL to a postcentral ROI.

We also defined 2 different types of functional ROIs within the anatomical ROI by selecting subsets of voxels with different functional properties on an individual-subject level. We defined the "functional finger ROI" as the region that best represented individual finger presses. To determine this region, we ran a volume-based searchlight on the set of voxels in each ROI. We again adjusted the radius of the searchlight for each center, such that either 80 (Experiment 1) or 160 voxels (Experiment 2) were included. We then selected the searchlight centers that were associated with the highest classification accuracy in each participant. For the selection of functional ROIs in Experiment 1, we averaged the accuracy of the ipsilateral and contralateral fingers for each voxel and then selected the voxels with the highest accuracy (top 20%, chosen because the hand region is roughly one-fifth of the surface of primary motor cortex) within each region. For the selection of functional ROIs in Experiment 2, we used the same approach, this time averaging the accuracies for the contra- and ipsilateral fingers during unimanual and bimanual presses and selecting the top 20% of voxels on these combined scores. Finally, we also defined a "functional bimanual ROI" by selecting the voxels with the 20% highest classification accuracies for the ipsilateral finger

during bimanual actions. Because these areas lay mainly on the boundary between primary and secondary motor areas, we used this method on a pre- and postcentral anatomical ROI.

Note that we did not use the ROI approach to make judgments of "whether" any regions significantly encoded finger presses in the first place. These tests were performed using multiple comparison corrections for the whole cortical surface. The functional ROI selection procedure was then performed to analyze "how" these regions encoded the finger presses. For example, we could compare within these ROIs between contra- and ipsilateral conditions for Experiment 1 and between contralateral, ipsilateral, unimanual, and bimanual conditions for Experiment 2. This is assured because these contrasts are orthogonal to the voxel-selection criterion, and the experimental design was fully balanced (Kriegeskorte et al. 2009). Also, any assessment of the correlation between left- and right-hand patterns can be made in an unbiased fashion, as the classification is performed independently for the 2 hands and selection is not biased toward specific patterns. For the decomposition analysis presented in Figure 7, we ensured through Monte-Carlo simulation that the selection criterion did not bias subsequent analyses.

COG Analysis

To determine whether there were significant differences in the location of the representations for ipsi- versus contralateral fingers, we determined the COG of the area with above-chance classification accuracy within the precentral and postcentral anatomical ROIs. Note that this approach differs from calculating the COG of the activation elicited by each finger (Indovina and Sanes 2001), a procedure that can test for a systematic somatotopic organization. Here, we ask whether the overall representation of ipsi- and contralateral finger presses was located in the same or different regions. The analysis was conducted on a flattened representation of the group surface. For each individual, we calculated the average spatial coordinates (x,y) for all vertices with above-chance accuracy (z-score >0), with each vertex weighed by the size of the z-score. Differences between center locations for ipsi- and contralateral accuracies were then tested across participants using a Hotelling's T2-test.

Pattern Component Analysis

Experiment 1. To assess the similarity of ipsilateral and contralateral finger patterns, we split each response pattern into an informative component (i.e. finger-related) and into a number of uninformative components (common activation patterns or noise). The correlation between patterns was then calculated on the informative part only. This method (Diedrichsen et al. 2011) allows the assessment of pattern similarity, while accounting for the influence of possible common activation patterns (which would increase correlations) and random trial-by-trial noise (which would decrease correlations). Using this technique, each observed pattern vector $y_{i,j,n}$ (ith hand, jth finger, and nth run) was decomposed into a common component for the hand h_i, finger f_j, and run r_n and a noise component $\varepsilon_{i,j,k}$. We estimated the variances of the left- and right-hand patterns and the covariance between them, as well as the variances of the finger patterns for each hand (σ_i^2) plus the average covariance between the 5 matching finger pairs (γ). Additionally, we estimated the variability of the component common to each run and of the trial-by-trial noise. The correlation between the ipsi- and contralateral finger patterns was calculated as:

$$r = \frac{\gamma}{\sqrt{\sigma_1^2 \sigma_2^2}} \tag{2}$$

Because these correlation estimates could become unstable if the variance associated with the finger patterns was very low, a very small constant (1e−5) was added to all finger variances.

Experiment 2. The purpose of the pattern component analysis for Experiment 2 was to determine how the ipsi- and contralateral patterns combined during bimanual actions. Therefore, we modeled the bimanual patterns ($y_{3,j,k,n}$, hand condition $i = 3$) as the sum of the pattern for the jth finger of the left hand ($b_{1,j}$), the pattern for the kth finger of the right hand ($b_{2,k}$), and an interaction term for the unique bimanual combination ($i_{j,k}$). Additionally, as effects of no interest, we allowed for a common bimanual activation pattern (b_3), a pattern common to all trials with a run (r_n) and a noise term ($\varepsilon_{3,j,k,n}$). As mentioned earlier, we modeled the activity patterns in the unimanual condition ($y_{i,j,n}$) as the sum of an activation pattern common to all fingers of the ith hand (b_i), a jth finger-specific pattern for that hand ($f_{i,j}$), a run-specific pattern (r_n), and a noise term for that trial. We estimated the variance of all of these components. We also estimated the covariance between the unimanual finger-specific patterns (f) and the corresponding bimanual finger-specific patterns (b). Of primary interest, however, was the size of the interaction term (i) and the main effect for the ipsilateral and contralateral fingers (b_1, b_2).

Removal of Mirror Movements from the Contralateral Hand

It is important to consider the alternative explanation that the ipsilateral finger representation was caused by subtle mirror movements of the contralateral hand, induced by uncrossed cortico-spinal projections. Such movements might lead to sensory-evoked activity, which could in turn be used to indirectly decode the presses of the ipsilateral fingers.

To monitor mirror movements, we instructed participants to exert light pressure with all fingers of both hands at all times on the response keys. Mirror contraction would then show up as subtle increases in the force produced by the matching fingers of the contralateral hand. Pilot experimentation indicated that this provided a more sensitive measure of mirror movements in the fMRI environment than electromyography. The force changes were then regressed out from the activity patterns, before submitting them to the classification analysis. If during ipsilateral actions the region only responded to the induced contralateral force changes, classification accuracy for the ipsilateral finger should be reduced to a guessing baseline.

To obtain unbiased results, we applied this approach in a cross-validated fashion: on each iteration of the cross-validation approach, we regressed the training data ($\mathbf{Y}^{\text{train}}$) against the forces produced in the ipsilateral ($\mathbf{Z}_{\text{ipsi}}$) hand and the (possibly) induced mirror movements in the contralateral ($\mathbf{Z}_{\text{contra}}$) hand. This regression was performed using the pattern component model, in which the variance of each component across voxels was estimated to regularize the estimation of the coefficients $\mathbf{u}$ (Diedrichsen et al. 2011):

$$\mathbf{Y}^{\text{train}} = \begin{bmatrix} \mathbf{Z}_{\text{ipsi}}^{\text{train}} & \mathbf{Z}_{\text{contra}}^{\text{train}} \end{bmatrix} \begin{bmatrix} \mathbf{u}_{\text{ipsi}} \\ \mathbf{u}_{\text{contra}} \end{bmatrix} + \varepsilon. \tag{3}$$

The 5 estimated pattern components related to the mirror movements ($\mathbf{u}_{\text{contra}}$) were then removed from the training and test data sets and the cleaned data submitted to the classification analysis:

$$\begin{aligned} \mathbf{Y}^{\text{train}*} &= \mathbf{Y}^{\text{train}} - \mathbf{Z}_{\text{contra}}^{\text{train}} \mathbf{u}_{\text{contra}} \\ \mathbf{Y}^{\text{test}*} &= \mathbf{Y}^{\text{test}} - \mathbf{Z}_{\text{contra}}^{\text{test}} \mathbf{u}_{\text{contra}} \end{aligned}. \tag{4}$$

Monte-Carlo studies showed that this method reduces the classification accuracy to chance level if the classification of the ipsilateral fingers is mediated fully through mirror movements in the contralateral hand.

We conducted a similar analysis for the bimanual condition of Experiment 2 to test the possibility that the nonlinear encoding of bimanual actions was caused by the fact that the presses of the contralateral hand were modulated in a nonlinear fashion by presses of the ipsilateral hand. Again, we regressed out the force changes in the contralateral hand from the activation patterns and then submitted the data to the classification analysis.

Results

Experiment 1: Unimanual Actions

We first determined the changes in the overall blood-oxygenation level-dependent (BOLD) response during contra- and ipsilateral finger presses. Figure 2*A* shows activation averaged over all fingers of each hand compared with the rest. For

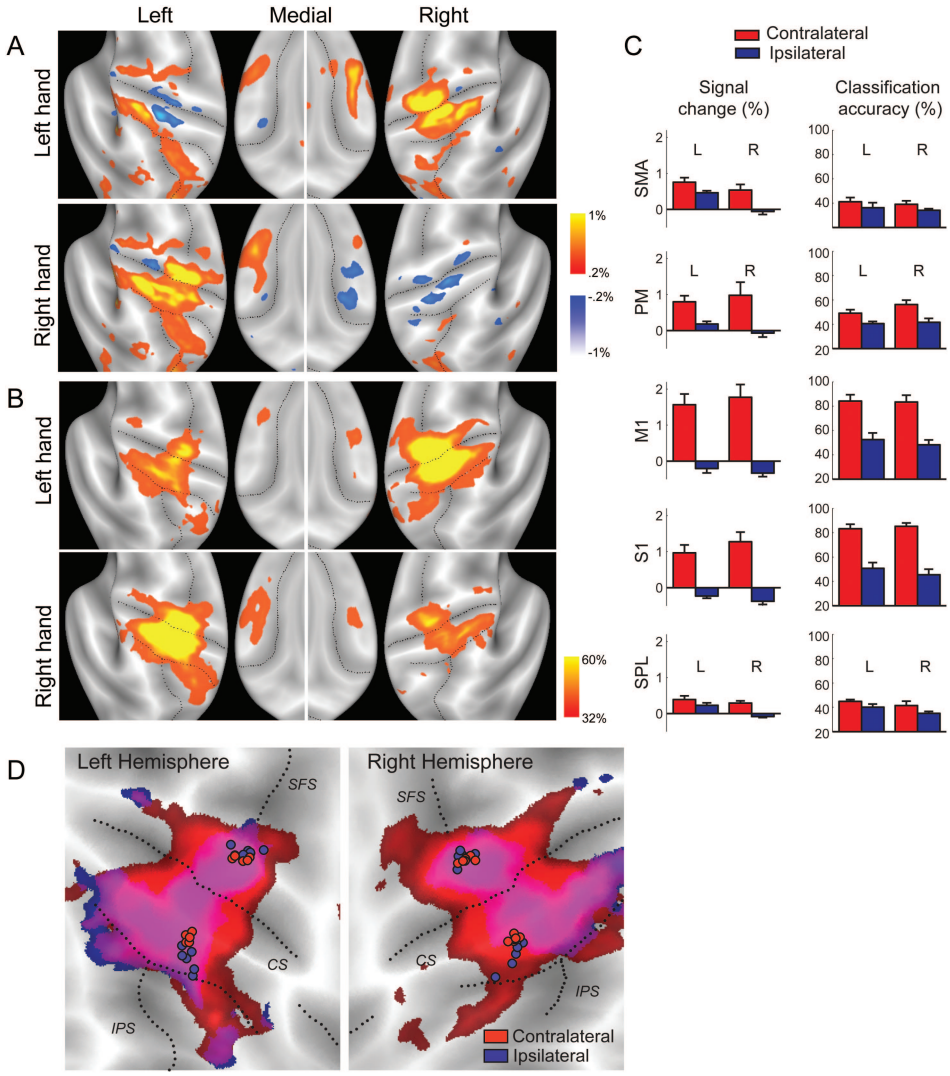

Figure 2. Representation of contra- and ipsilateral finger presses in the human neocortex. (*A*) Group-average percent signal change (threshold ±0.2%) averaged over all fingers and compared with rest. During ipsilateral actions, suppression can be observed in primary sensory and motor cortices. Positive activation during ipsilateral finger presses can be observed in the left hemisphere. (*B*) Classification accuracy, thresholded at >32%, $Z > 1.97$. Colored regions show local voxel patterns that significantly distinguish between different fingers. High classification accuracy for ipsilateral presses can be found in regions that are deactivated compared with the rest. (*C*) Mean signal change and classification accuracy for contralateral (red) and ipsilateral (blue) finger presses in the informative region within 5 anatomically defined ROIs of the left (L) and right hemispheres (R). Error bars indicate across-subject SE. (*D*) Overlap of classification accuracy (>32%) for contralateral (red) and ipsilateral (blue) fingers. Circles indicate the COG of classification accuracy for individual participants for precentral and postcentral ROIs. CS, central sulcus; SFS, superior frontal sulcus.

contralateral finger presses, we found activation in a set of regions including the hand area of primary motor cortex (M1), primary sensory cortex (S1), PM, the SMA, and SPL.

Significant overall signal changes (corrected for multiple tests, Table 1) were also observed during ipsilateral presses. "Decreases" in overall activity were found in both hemispheres in the primary sensory and motor cortices. Significant signal "increases" were observed in ipsilateral PM (Cramer et al. 1999; Hanakawa et al. 2005; Verstynen et al. 2005; Horenstein et al. 2009; Verstynen and Ivry 2011) and SMA. Consistent with previous results (Kim et al. 1994; Verstynen et al. 2005), we found that these activity changes were asymmetric across hemispheres. Figure 2*C* shows the percent signal change in the functional finger area of the 5 anatomical ROIs (see Materials and Methods). Whereas the BOLD signal for contralateral presses (left or right) was similar in left and right hemispheres [all $t(5) < 1.59$, $P > 0.17$], the BOLD signal for ipsilateral presses was always higher in the left hemisphere. The difference between hemispheres did not reach significance in M1 [$t(5) = 2.091$, $P = 0.09$] or S1 [$t(5) = 2.091$, $P = 0.09$], but was significant for PM [$t(5) = 3.531$, $P = 0.017$], the SMA [$t(5) = 5.924$, $P = 0.002$], and SPL [$t(5) = 3.426$, $P = 0.019$]. In sum, these results replicate previous findings of systematic BOLD signal decrease in the primary hand area (Talelli, Ewas et al. 2008) and increases in slightly more anterior regions, especially in the left hemisphere (Kim et al. 1993; Verstynen et al. 2005).

Encoding of Contra- and Ipsilateral Fingers

We then asked whether the activation changes related to ipsilateral finger presses reflect a nonspecific response or whether the neural activity encodes specific movement

Table 1
Areas showing significant BOLD signal increases or decreases in Experiment 1 during ipsilateral finger presses

Name	Peak *t*-value	Area (mm^2)	*P* (corr.)	*x* (mm)	*y* (mm)	*z* (mm)
Ipsilateral movement > rest						
Left SMA	8.75	214	0.001	−5.79	−2.12	58.87
Left PM	12.5	97	0.023	−41.42	−4.09	43.69
Ipsilateral movement < rest						
Left M1/S1	−18.59	216	0.001	−33.53	−23.80	46.11
Right SI	−116.38	274	0.000	46.64	−17.69	52.07
Right M1	−8.24	86	0.025	27.29	−21.99	61.20
Right M1	−14.68	87	0.001	44.30	−9.39	34.67
Right SPL	−14.77	125	0.035	27.48	−42.01	53.02

Note: Only clusters that are significantly corrected for multiple tests over the sensory motor areas (M1, S1, PM, SMA, and SPL) of the hemisphere are shown. At an uncorrected threshold of $t(5) < -4.03$, $P = 0.005$, the critical cluster size for $P < 0.05$, family-wise error-corrected, is 75.4 mm^2. The peak *t*-value, the size of the area in mm^2, and the cluster-corrected *P*-value are listed. *x*-, *y*-, and *z*- coordinates are reported for the location of the local maxima on the average Freesurfer surface, which was aligned to the Montreal Neurological Institute atlas.

Table 2
Surface clusters that show significant classification accuracy for ipsilateral actions in Experiment 1

Region	Peak *t*-value	Area (mm^2)	*P* (cl.)	*x* (mm)	*y* (mm)	*z* (mm)
Left S1	17.75	1570	0.000	−45.44	−26.44	37.27
Left M1	21.16	522	0.001	−35.68	−11.42	59.90
Left SPL	12.34	433	0.001	−21.86	−61.67	57.73
Right M1/S1	25.62	1741	0.000	29.55	−28.61	48.79
Right SMA	17.11	429	0.001	8.69	−11.39	62.37
Right SPL	19.44	408	0.001	23.03	−58.07	52.05

Note: Only clusters that are significantly corrected for multiple tests over the cortical surface of the hemisphere are shown. At an uncorrected threshold of $t(5) > 4.03$, $P = 0.005$, the critical cluster size for $P < 0.05$, corrected, is 107 mm^2.

parameters (i.e. the specific finger pressed). Multivoxel pattern analysis can detect such representations by testing for systematic differences in the local activity patterns for different task conditions. The strength of the method is that it can detect task-relevant representations, even if these do not have a systematic somatotopic organization, or fall below the spatial resolution of fMRI (Kamitani and Tong 2005, 2006; Swisher et al. 2010; Wiestler et al. 2011). Using a surface-based searchlight approach (Kriegeskorte et al. 2006; Oosterhof et al. 2011), we tested for the presence of ipsi- and contralateral finger representations anywhere on the cortical surface (Fig. 2*B*).

As expected, contralateral finger representations were found in the hand area of M1 (Yousry et al. 1997) and in an extended region of S1, with average classification accuracies in the informative regions (see Materials and Methods for definition) reaching 84% (Fig. 2*C*). Furthermore, the area of significant classification accuracy extended into the dorsal PM, the SPL, and the SMA. Thus, consistent with other results (Indovina and Sanes 2001; Maier et al. 2002; Wiestler et al. 2011), we found evidence for representations of individuated finger movements in multiple contralateral cortical regions.

Surprisingly, however, the same regions that had a representation of the contralateral finger also encoded finger presses of the ipsilateral hand. The average classification accuracy in the functional finger area was 48% for M1 and 50% for S1. The representation of ipsilateral finger movements was clearly visible in each individual participant (Supplementary Fig. S1) and was significant after correcting for multiple tests across the cortical surface in all regions, including the SMA and parietal cortex (Table 2). It is noteworthy that the representation was "not" centered on regions that showed activity increases with ipsilateral finger presses. The strongest representation of ipsilateral fingers was found in regions in primary sensory and motor cortices, that showed negative or no "overall" signal change during ipsilateral actions compared with the rest. This indicates that there can be systematic and informative variations of the BOLD signal, even if the overall mean activity is below or close to zero (see also Wiestler et al. 2011). In contrast, when we selected a functional ROI in PM that was defined by the voxels that showed the highest activity increases during ipsilateral presses, classification accuracy was appreciably lower (28.4%, SD = 0.043%).

The areas that encoded ipsilateral finger presses also overlapped nearly perfectly with the areas that encoded contralateral fingers (Fig. 2*D*). To test this observation quantitatively, we determined the COG (see Materials and Methods) of the above-chance classification accuracy for each participant for the precentral and postcentral anatomical ROIs. We then tested whether the COG locations were significantly different for ipsi- and contralateral presses. For the precentral ROI, we found no significant differences in either the right [$T^2(2,4) = 12.20$, $P = 0.08$] or left hemisphere [$T^2(2,4) = 3.292$, $P = 0.36$]. For the postcentral ROI, there was a significant posterior shift in the ipsilateral compared with the contralateral representation in both the left [$T^2(2,4) = 83.80$, $P = 0.003$] and right hemispheres [$T^2(2,4) = 23.64$, $P = 0.03$].

Thus, while a subtle spatial gradient could be observed in the postcentral ROI, our results indicated that contra- and ipsilateral finger presses were largely encoded in the same areas. The ipsilateral representation was centered on regions whose mean activity decreased overall during ipsilateral presses, rather than on the more anterior regions where mean activity increased.

Similarity Analysis: Contra- and Ipsilateral Finger Maps are Highly Correlated

Our spatial analysis shows that the representations of contra- and ipsilateral finger presses overlap greatly. This could occur in several ways: Figure 3*A* illustrates how a set of hypothetical finger patches, that is, groups of neurons that preferentially respond during presses of contra- and ipsilateral fingers, could be arranged in the hand area of 1 hemisphere. In one extreme, the ipsilateral patches are closely interdigitated with the contralateral patches in such a way that there is no relationship between the tuning for individual fingers (uncorrelated representations). In the other extreme, ipsilateral movements would activate the very same cortical patches that are involved in the control of the contralateral presses (identical representations). In an intermediate scenario, contra- and ipsilateral finger patches are independent, but are arranged in a spatially correlated manner (correlated representation). The latter 2 arrangements would predict that we should find a high correlation between the activity patterns elicited by movements of contra- and ipsilateral fingers.

To illustrate the relationship of the activation patterns graphically, we selected the functional finger ROI of M1 (see Materials and Methods) and split its voxels into 5 groups, depending on the contralateral finger for which they showed the highest activity (Fig. 3*B*, left). For example, we labeled all voxels that showed higher activity for the thumb compared

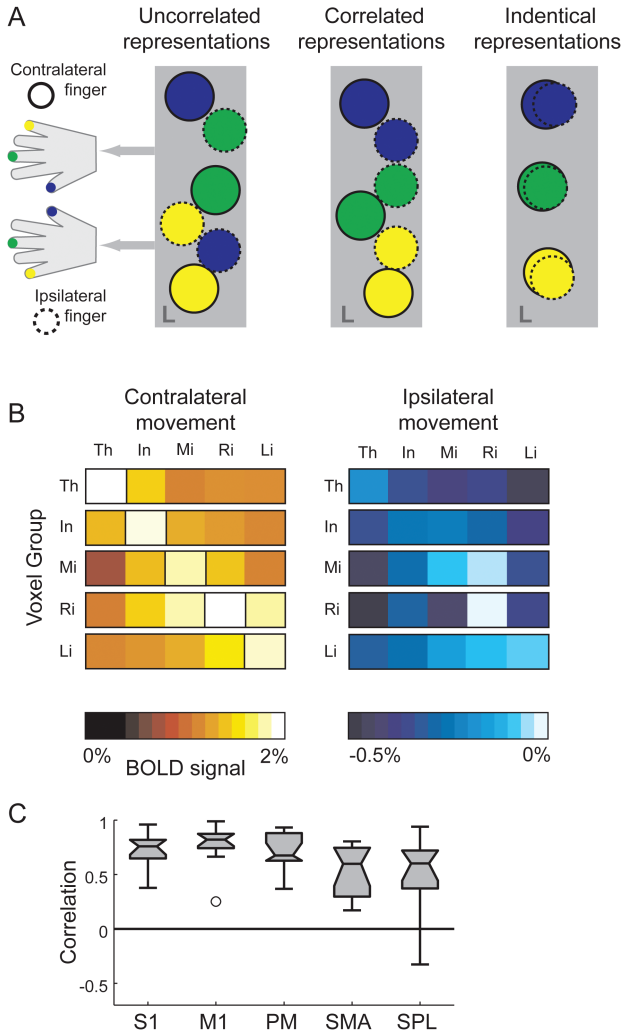

Figure 3. Similarity analysis between ipsilateral and contralateral finger representations. (*A*) Three hypothetical arrangements of finger patches: small regions of cortex that are preferentially activated for one of the contralateral (solid circles) or ipsilateral (dashed circles) fingers. Note that activation patches for individual fingers in M1 are highly overlapping; the distinct patches are for illustration only. Uncorrelated representations: patches for ipsi- and contralateral fingers are distinct and arranged in an interdigitated but uncorrelated fashion. Correlated representations: distinct patches, although patches responding to ipsilateral finger movements are always near patches responding to the corresponding contralateral fingers. Identical representations: ipsilateral movements activate the same patches as the corresponding contralateral finger. The latter 2 architectures would lead to a high spatial correlation of ipsilateral and contralateral patterns. (*B*) Percent signal change in the hand area of primary motor (averaged over hemispheres and individuals) for contra- and ipsilateral finger presses. Data are split into 5 groups of voxels according to the contralateral finger for which the voxels showed the maximal activation (left, highlighted diagonal in matrix). For ipsilateral actions (right), voxel groups tend to show the highest activation, below a global suppression, for movements of the mirror-symmetric ipsilateral finger. (*C*) Voxel-by-voxel correlation between the contralateral and ipsilateral finger patterns, corrected for overall noise and common activation patterns. The box plot extends from the 25th to the 75th percentile. Whiskers indicate the full range of the data. Outliers (indicated by circles) are data points that are more than 1.5 times the box length away from the median.

with all other fingers as "thumb voxels." We then analyzed the activity of these voxel groups for ipsilateral finger presses (Fig. 3*B*, right). Although all 5 voxel groups showed suppression, most of the groups showed relatively higher activation for the same fingers during contra- and ipsilateral presses. For example, the thumb voxels (first row) had the highest activity during ipsilateral thumb presses, that is, suppression was lowest for this condition. Thus, below the general suppression of the BOLD signal in the ipsilateral motor cortex, we found an activity pattern similar to that observed during presses of the corresponding contralateral fingers.

To quantify the correlation between the contra- and ipsilateral representation, we employed a new pattern-decomposition method (Diedrichsen et al. 2011). Using this method, we decomposed the contra- and ipsilateral activity patterns into a component that was informative about which of the 5 fingers moved and 2 noninformative components: a common nonspecific component and noise. This allows us to calculate the correlation between the informative parts of the ipsi- and contralateral patterns, independent of noise levels or a common activation pattern shared by all contra- and ipsilateral activations. The resultant correlation coefficients, therefore, indicate the degree to which finger-specific patterns for ipsilateral fingers are explained by the contralateral finger-specific representation. The mean correlation coefficient (Fig. 3*C*) was 0.83 (range 0.45–0.90) for M1. Similarly, high correlations were found for S1 ($r = 0.77$) and PM ($r = 0.75$), with lower correlations in SMA ($r = 0.57$) and SPL ($r = 0.54$). Notably, the premotor region that increased activity with ipsilateral movements (Verstynen et al. 2005; Verstynen and Ivry 2011) also showed a substantial correlation between contra- and ipsilateral activity patterns ($r = 0.60$). Thus, the neural pattern that informed us about the ipsilateral finger was well predicted (70% for the primary motor cortex) by the activity patterns observed by the corresponding contralateral finger. Our results, therefore, argue that ipsi- and contralateral actions activate the same patches or that the activated patches are at least spatially correlated (Fig. 3*A*).

Additional analyses show that these patterns were not caused by overt mirror movements of the contralateral hand. Mirror movements should be apparent in slight force increases in the mirror-symmetric finger that was pressed on the other hand. We monitored these by instructing participants to keep both hands placed on the keyboard and exert a light constant pressure with all 10 fingers. We detected significant contralateral increases ($P < 0.05$, uncorrected) for presses of the 4th and 5th digits. However, these increases averaged 0.011 N for the ring and 0.025 N for the little finger, well below 1% of the average force increase in the instructed hand (3.46 N). For the other 3 fingers, no significant mirror movements were observed. However, the cortical activation patterns distinguished between digits 1 and 3 (average pairwise $d' = 3.55$) better than between digits 4 and 5 (pairwise $d' = 3.12$). We also show that if we remove the influence of force changes on the contralateral hand (see Materials and Methods), the classification accuracy for the ipsilateral fingers across all functional finger ROIs was reduced by <1%. Therefore, we conclude that the observed mirror movements were a consequence of strong cortical mirror activation. Our results clearly argue against the alternative interpretation that the cortical activation patterns are merely a consequence of sensory re-afference from mirrored muscle contractions induced by uncrossed cortico-spinal innervations or other spinal mechanisms.

To summarize, Experiment 1 showed that when people make individuated finger movements, 2 processes occur in ipsilateral cortical motor regions. First, in many areas, the BOLD signal is generally suppressed, most likely relating to a suppression of synaptic activity (Shmuel et al. 2002, 2006).

Secondly, below this suppression, there is a finger-specific activation of the same voxels that are activated by the mirror-symmetric contralateral finger press. This mirrored representation, although weaker, was also found in the premotor area that showed increased activity during ipsilateral actions.

Experiment 2: The Ipsilateral Mirror Representation Disappears During Bimanual Actions

The high correlation between patterns for ipsi- and contralateral fingers found in Experiment 1 suggests that ipsilateral finger presses activate the same patches that are active during contralateral finger presses (Fig. 3*A*, identical representation). However, it may also be true that the representations are independent, but arranged in a spatially correlated fashion (correlated representations). The limited spatial resolution of fMRI would then give the impression of highly similar patterns.

In Experiment 2, we thought to dissociate these 2 possibilities by studying how the representations of ipsi- and contralateral fingers interact during bimanual actions. If ipsilateral actions activated the same circuits involved in contralateral control, then this would cause problems if one were to execute an asymmetric bimanual action. In this situation, we therefore predict that the ipsilateral finger representations should be suppressed by the ongoing activity related to the contralateral hand. If, however, the ipsilateral and contralateral representations relied on different neuronal circuits, then both should remain visible during bimanual actions.

Participants were instructed to make unimanual or bimanual finger presses. In the unimanual condition, participants had to press 1 of 3 the fingers (digit 1, 3, or 5) of the left or right hand (Fig. 4*A*). In the bimanual condition, all 9 possible combinations of these fingers were tested (Fig. 4*B*). We then used 3 separate classifiers to identify regions that showed finger-specific patterns: 1 for left unimanual actions, 1 for right unimanual actions, and 1 for bimanual actions. The latter classifier was trained to distinguish between the 9 unique combinations of bimanual finger presses, independent of the fingers involved in the combination.

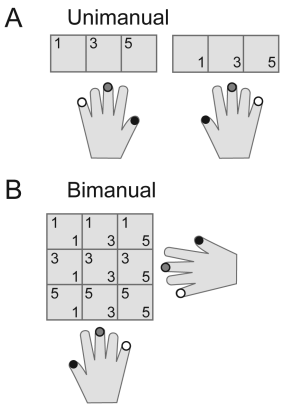

Figure 4. Methods for Experiment 2. (*A*) In the unimanual condition, we tested 3 fingers for each hand. Separate classifiers were used to detect representations of contra- and ipsilateral fingers. (*B*) In the bimanual condition, all 9 combinations of the left and right fingers were tested. A single bimanual classifier was trained to distinguish between these 9 combinations. By comparing the true bimanual combination with the classifier's prediction, we could then determine whether the fingers of the contra- and/or ipsilateral hand were decoded correctly.

By comparing the true bimanual action with the action that the classifier predicted, we could then determine how strongly the pattern reflected the contra- and/or ipsilateral finger. For example, if the true finger combination involved both thumbs (cell 1,1, Fig. 4*B*), then any classifier prediction falling into the first column would imply correct contralateral classification and any prediction in the first row would imply correct ipsilateral classification. Thus, while ipsi- and contralateral fingers were inherently decoded together, we could nevertheless determine the strength of the ipsi- and contralateral representations during bimanual actions separately.

For the unimanual condition (Fig. 5*A*, upper row), we replicated Experiment 1: large areas of the sensory motor cortex encoded the ipsilateral action (Table 3, unimanual). Again, these regions were nearly identical to those encoding the contralateral finger presses (data not shown).

What would we now expect to see in the bimanual condition? If independent sets of neurons responded to contra- or ipsilateral actions, then the ipsi- and contralateral pattern should combine in the bimanual condition. Simulations based on the assumption of independent representations would combine in an approximately linear fashion (see Supplementary Material for details), predicted that we should observe an equal decrease in both the contra- and ipsilateral classification accuracies (Fig. 5*B*).

The data clearly fail to support this prediction. In the functionally defined finger ROIs of the primary sensory and motor cortices (Fig. 5*C*), the classification accuracy for the contralateral finger was comparable across unimanual and bimanual conditions, all $t(6) < 1.763$, $P > 0.128$. In contrast, the ipsilateral representation disappeared almost completely in the bimanual condition (Fig. 5*A*, lower row). Compared with the unimanual condition, the accuracy for the ipsilateral finger was significantly reduced in M1 [$t(6) = 4.288$, $P = 0.005$] and S1 [$t(6) = 4.902$, $P = 0.003$]. Thus, the classifier accurately decoded the contralateral finger during bimanual actions, but performed nearly at chance levels for the ipsilateral finger. Thus, the data are clearly at odds with linear superposition of patterns. In the additional analysis, we show that the reduction in accuracy cannot be explained by signal-dependent increases in noise or a nonlinearity between neural activity and the BOLD signal (Supplementary Material).

These findings, therefore, indicate that the strong encoding of ipsilateral actions found in the unimanual condition truly disappears during bimanual actions. This conclusion is further supported by a pattern decomposition analysis (discussed subsequently). Thus, our results argue against independent representations of contra- and ipsilateral fingers in the primary motor cortex. Rather, it seems that if one motor cortex is not involved in the control of a contralateral action, ipsilateral finger presses lead to the activation of exactly those circuits that would normally be involved in the mirror-symmetric finger press. When both hands are functionally engaged, the contralateral action dominates the local activity pattern.

A Different Type of Ipsilateral Representation for Bimanual Actions

There were, however, regions from which the classifier could decode both the contra- and ipsilateral fingers during bimanual actions. Such activity was present in both hemispheres on the boundary between M1 and PM and in the anterior parietal lobule (Fig. 5*A*, lower row). Although the encoding was

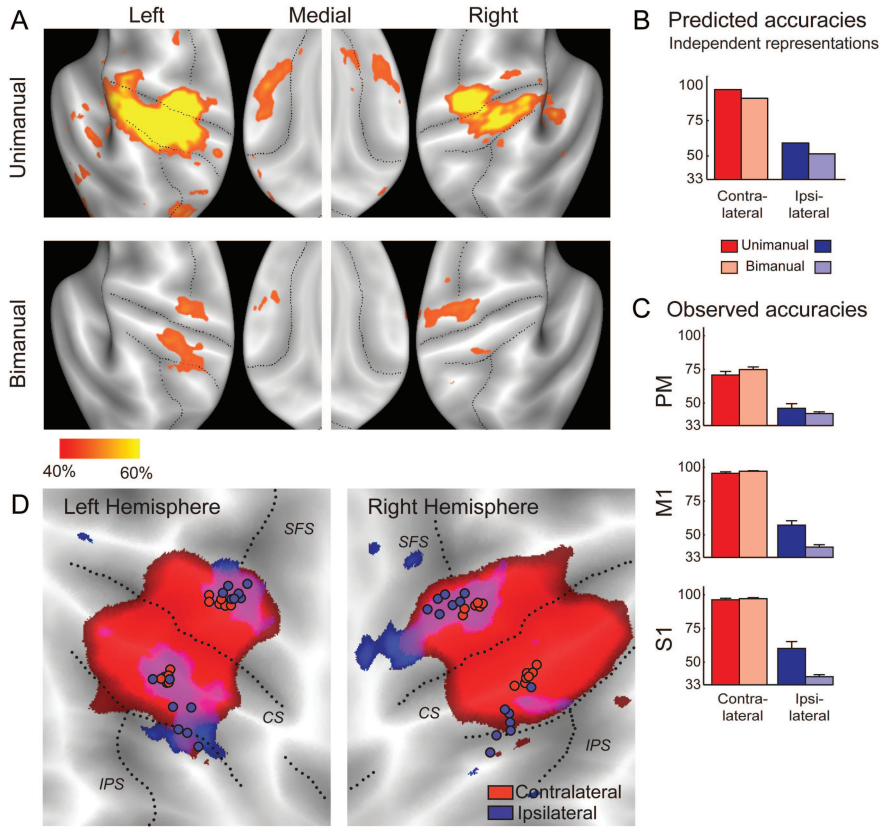

Figure 5. Representations of ipsilateral fingers during unimanual and bimanual actions. (*A*) Surface maps of the classification accuracy for the ipsilateral finger (40% accuracy threshold, $Z = 1$) during unimanual (upper row) and bimanual (lower row) finger presses. (*B*) Predicted accuracies, assuming that contra- and ipsilateral patterns superimpose linearly. (*C*) Observed classification accuracy in informative subregions (see Materials and Methods) of 3 anatomical ROIs for contralateral (red) and ipsilateral (blue) fingers. Results are averaged across the 2 hemispheres. Error bars represent across-subject standard error of the mean. (*D*) Spatial relationship of areas encoding the contralateral (50% threshold, red) and ipsilateral fingers (40% threshold, blue) during bimanual actions. Circles indicate the individual COGs of the functional finger ROI of the precentral and postcentral gyri. CS, central sulcus; SFS, superior frontal sulcus.

Table 3
Cortical areas that show significant classification accuracy for the ipsilateral fingers during unimanual and bimanual actions in Experiment 2

Location	Peak *t*-value	Area (mm^2)	*P* (cl.)	*x* (mm)	*y* (mm)	*z* (mm)
Unimanual						
Left M1/S1	7.11	1284	0.000	−31.43	−21.27	44.83
Right S1	8.94	547	0.001	44.76	−26.56	46.42
Right M1	8.71	388	0.004	38.49	−12.23	63.13
Bimanual						
Left PM	12.81	561	0.000	−27.00	−16.17	66.54
Left SPL	7.40	328	0.003	−31.58	−36.12	56.53
Left SPL	10.01	173	0.037	−39.34	−41.27	38.66
Left parietal	11.20	216	0.016	−60.27	−28.55	20.78
Operculum						
Right PM	15.82	1004	0.000	30.64	−15.33	61.38
Right SPL	14.37	169	0.024	28.75	−59.17	46.82

Only clusters that are significantly corrected for multiple tests over the cortical surface are shown. At an uncorrected threshold of $t(6) > 3.707$, $P = 0.005$, the critical cluster size for $P < 0.05$, corrected, is 159 mm^2.

weaker than that found during unimanual actions, it was significant in both hemispheres after correcting for multiple tests (Table 3, bimanual).

Our results indicate that this bimanual finger representation differed fundamentally from the ipsilateral finger representation observed during unimanual actions. At first glance, this difference is apparent in the spatial locations of the regions that coded for contra- and ipsilateral fingers (Fig. 5*D*). For bimanual actions, the ipsilateral finger representation was located further away from the central sulcus than the contralateral representation. In the anatomically defined precentral ROI, the individual COGs for the ipsilateral fingers were more anterior than those for the contralateral fingers [left hemisphere: $T^2(2,5) = 44.82$, $P < 0.0048$ and right hemisphere: $T^2(2,5) = 48.74$, $P < 0.004$). Similarly, in the postcentral gyrus, the ipsilateral COGs were located more posterior [left: $T^2(2,5) = 19.37$, $P = 0.027$ and right: $T^2(2,5) = 37.13$, $P = 0.0072$]. In contrast, a similar spatial analysis for unimanual actions did not yield a significant difference for the precentral gyrus, replicating the results of Experiment 1. Finally, a direct comparison of the area encoding ipsilateral fingers during bimanual and unimanual actions showed that the COGs differed significantly in the right precentral [$T^2(2,5) = 34.48$, $P = 0.008$] and postcentral ROIs [$T^2(2,5) = 32.75$, $P = 0.009$] and were marginally different for the left precentral [$T^2(2,5) = 8.227$, $P = 0.115$] and postcentral ROIs [$T^2(2,5) = 7.625$, $P = 0.128$]. These results indicate that the mirrored ipsilateral finger representation during unimanual actions is located predominantly in caudal or "new" M1, whereas the ipsilateral finger representation for bimanual actions is shifted toward the rostral or "old" M1 (Rathelot and Strick 2009) and caudal PM.

Encoding of Bimanual Actions Relies on Elements with Nonlinear Tuning

If the identified ipsilateral region is functionally engaged in the control of coordinated bimanual movements, we hypothesize that it should represent bimanual finger presses jointly. Consider the example of playing a tune on the piano. Imagine that you need to accentuate a combination of notes played jointly with the left thumb and the right middle finger (Fig. 6*A*,*B*, cell A) and another combination of notes played by the left middle finger and right little finger (cell B). All other combinations of the same fingers (cells C and D) should not receive the same stress. If the motor system had only neural units with tuning functions reflecting a linear combination of the left- and right-hand actions, such a task could not be learned. For example, any change to the output of a unit that is mostly activated during bimanual combination A would generalize to bimanual actions C and D (Fig. 6*A*). To produce different amounts of force for arbitrary combinations of bimanual movements, the motor system, therefore, needs neural circuits that show nonlinear tuning for bimanual actions (Fig. 6*B*; Yokoi et al. 2011). One example would be patches of cortex that responded preferentially to a single specific bimanual combination. However, any sufficient set of arbitrary nonlinear tuning functions would allow the nervous system to learn arbitrary functions of 2 variables (Zipser and Andersen 1988; Pouget and Sejnowski 1997).

How can we determine whether the activity patterns related to ipsi- and contralateral finger movements combine linearly or nonlinearly? To illustrate the analysis, we visualized the tuning properties of voxels for uni- and bimanual actions in the functional bimanual ROI of the precentral regions (see Materials and Methods and Fig. 6*C*). We split these voxels into 9 groups, based on the bimanual condition for which a voxel showed the highest activity (black cross). Each 3 × 3 matrix now shows the average activity of these 9 voxel groups in the unimanual and bimanual conditions.

Consistent tuning for finger presses for 1 hand can be determined by averaging the bimanual tuning functions across the fingers of the respective other hand (Fig. 6*C*, arrows). A consistent representation would be evident in differences between these averaged patterns. We can quantify the strength of each of these main effects by estimating the variance of the corresponding pattern component (see Materials and Methods, Diedrichsen et al. 2011), a measure analogous to the sum of squares in a traditional 2-factorial univariate analysis of variance (ANOVA).

For the main effect for the contralateral fingers, the variance estimates were relatively large and equal across unimanual and bimanual conditions (Fig. 7*A*), indicating strong and consistent encoding of this variable. This consistent tuning can even be seen in the tuning functions when averaging within rows (Fig. 6*C*). From this figure, it is also apparent that the consistent bimanual tuning was very similar to the tuning during contralateral unimanual actions. Indeed, the correlation between the informative part of the unimanual and bimanual patterns was nearly one for both the pre- and the postcentral ROIs (Fig. 7*C*). Thus, the tuning for the contralateral finger in the bimanual condition can be nearly perfectly predicted by the tuning in the unimanual condition.

In contrast, the variance estimate for the ipsilateral fingers in the bimanual condition was much lower than that in the

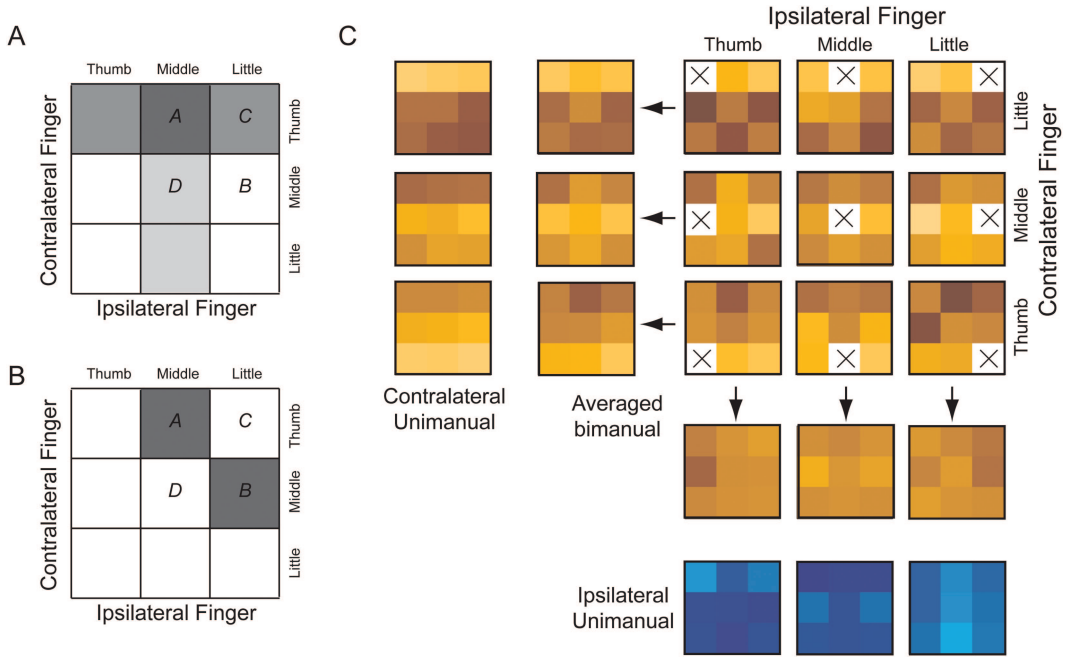

Figure 6. Nonlinear tuning of voxels for bimanual actions. (*A*) Tuning function of a hypothetical neural unit for the 9 task conditions of a bimanual task. The activity of this unit (indicated by the gray shading) is determined by a linear combination of a tuning function for the ipsi- and contralateral fingers. Any change in the units output would influence task condition A mostly, but would generalize to conditions C and D. A system that has only linear units could, therefore, not learn a task in which a different output has to be produced for combinations A and B than for bimanual finger combinations C and D. (*B*) Instead, the control of such a task requires cortical circuits with nonlinear combinations of contra- and ipsilateral actions. (*C*) Average tuning functions of the voxels in the functional bimanual ROI in precentral gyrus, averaged across hemispheres and participants. Each 3 × 3 matrix indicates the activity of 9 groups of voxels, which were selected based on the bimanual combination for which they are most highly activated (black cross). The activity in the other conditions can then be averaged across the contralateral or ipsilateral finger to reveal the presence of consistent tuning across the bimanual actions. For the contralateral finger, this tuning is highly similar to the one observed for unimanual actions. For the ipsilateral finger, no tuning is apparent. Nonlinear tuning would be apparent as an interaction effect in this 2-factorial design.

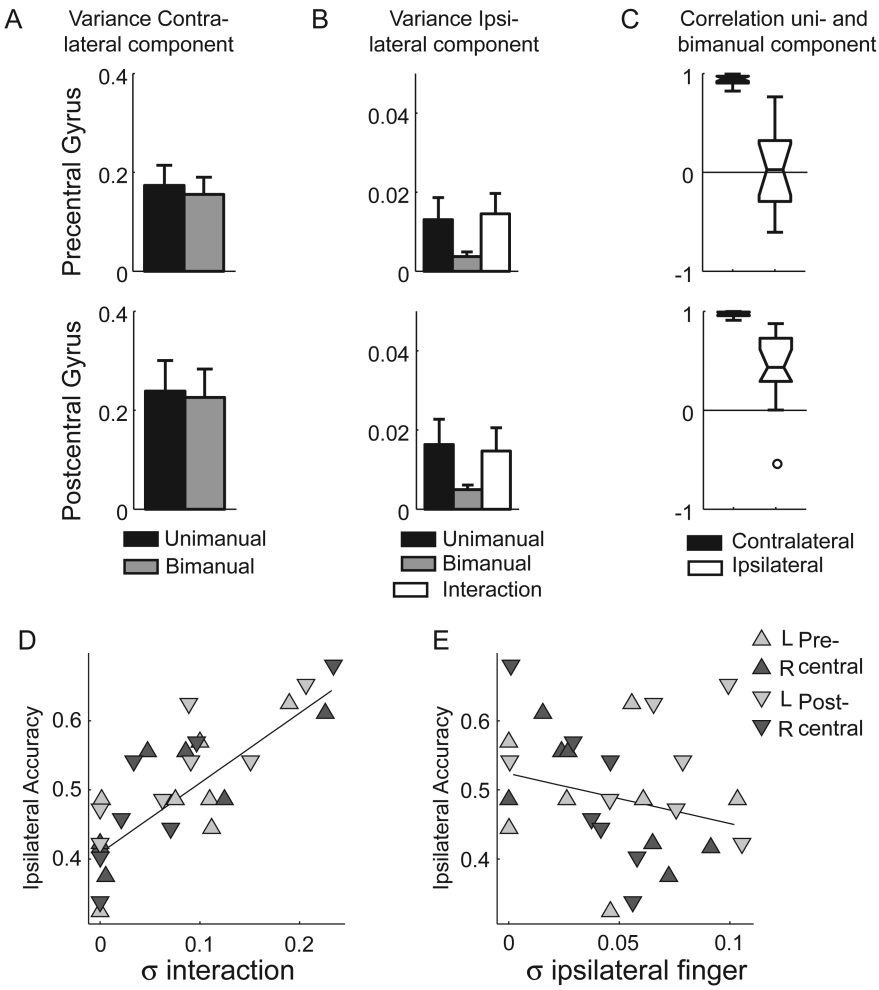

Figure 7. Pattern decomposition shows clear evidence for nonlinear bimanual tuning of voxels in the functionally defined bimanual ROI in pre- and postcentral gyri. (*A*) For the bimanual patterns, the variance estimate for the contralateral component is relatively strong and equivalent for uni- and bimanual movements. (*B*) The variance of the ipsilateral component effect is reduced for the bimanual movement compared with unimanual. However, a substantial interaction effect between ipsi- and contralateral fingers (white bar) is observed. (*C*) For contralateral fingers (red), there is a high correlation between the unimanual and bimanual pattern components of the same finger. For ipsilateral finger presses (blue), there is no systematic relationship. Box plots extend from the 25th to the 75th percentile. Whiskers indicate the full range of the data, with circle indicating data points that are further away from the median than 1.5 the times the box length (intraquartile range). (*D*) The classification accuracy for the ipsilateral finger during bimanual actions correlates with the size of the interaction effect. Values for the bimanual area within the left and right precentral and postcentral ROIs are shown for each participant. (*E*) Classification accuracy does not correlate with the size of a pattern component related to the ipsilateral main effect. Error bars indicate between-participant SE.

unimanual condition (Fig. 7*B*). This reflects the observation that the voxels showed no consistent tuning for the ipsilateral fingers when averaging the bimanual activity along the columns (Fig. 6*C*). It also confirms the results of the classification analysis (Fig. 5*A*), again showing that the consistent tuning for ipsilateral actions disappears in the bimanual context.

Importantly, neuronal circuits that show nonlinear tuning for ipsi- and contralateral fingers would become evident in an interaction effect between the 2 main factors. Indeed, a substantial part of the pattern variance in the bimanual condition was explained by the nonlinear interaction term (Fig. 7*B*, white bar). This finding indicates that the ipsilateral action modulated the activity of voxels in a way that depended nonlinearly on the contralateral action. Across subjects and pre- and postcentral regions, the interaction effect predicted the classification accuracy for ipsilateral finger during bimanual actions ($r = 0.837$, $P < 0.001$, Fig. 7*D*), whereas the estimated strength of the ipsilateral main effect did not ($r = -0.25$, $P = 0.193$, Fig. 7*E*). Thus, we can conclude that the observed classification accuracy for the ipsilateral finger during bimanual actions depended on neural circuits with nonlinear tuning for ipsi- and contralateral actions.

What is the source of this nonlinear encoding? First, we considered the possibility that the neural areas involved in producing bimanual actions were more activated during asymmetric actions (trials with different fingers) than during symmetric actions (trials with the same fingers). Such an effect would indeed lead to an interaction between the contra- and ipsilateral fingers. Many prior imaging studies have found more activity during asymmetric than during symmetric movements in the SMA, PM, and the SPL (Debaere et al. 2001; Ullen et al. 2003; Wenderoth et al. 2004, 2005; Diedrichsen et al. 2006). Consistent with these studies, we found areas in the superior frontal sulcus and along the IPS that were more activated during asymmetric actions (Fig. 8, green). This effect, however, was spatially completely separate from areas that encoded the bimanual action (Fig. 8,

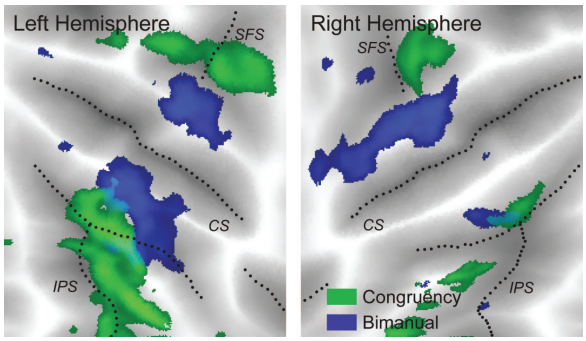

Figure 8. Areas that show an effect of bimanual congruency (green) and bimanual finger encoding (blue) do not overlap. Green areas are activated more during asymmetric than during symmetric movements (threshold: 0.07% signal change), and blue areas show above-chance classification accuracy for the ipsilateral finger during bimanual actions (40% threshold). An effect of congruency was found in the depth of the IPS and superior frontal sulcus (SFS), whereas the encoding of bilateral finger movements is more closely located to the central sulcus (CS).

blue). Furthermore, in the bimanual (blue) regions, no difference between symmetric and asymmetric activity patterns could be found; the classifier could distinguish equally well between 2 patterns associated with asymmetric trials, as between symmetric and asymmetric patterns. Thus, the nonlinear encoding of bimanual finger combinations and the encoding of the congruency of bimanual actions were independent.

Secondly, we tested the idea that the nonlinear tuning may not reflect direct encoding of the ipsilateral action, but instead reflects the indirect influence of small, but systematic, behavioral changes in the contralateral hand. Indeed, in a 2-factorial ANOVA with the maximal force as the dependent variable and the ipsi- and contralateral fingers as the 2 independent factors, we observed small but significant interaction effects in 5 out of 14 hands, across 3 of the 7 participants. However, by regressing these contralateral force changes out of the activity patterns before classification (see Materials and Methods), we could show that this information contributed only minimally to the encoding of the ipsilateral finger. After correction, the classification accuracy changed from 43% to 41%, a nonsignificant difference [$t(6) = 1.786$, $P = 0.124$]. Even after the correction, the areas still showed significant encoding of the ipsilateral finger presses [$t(6) = 4.894$, $P = 0.001$].

Instead, we argue that the nonlinear encoding of the bimanual finger representation reflects neuronal elements that are used to control bimanual actions. To be useful for control, this population of neural circuits should code for any possible combination of movements of the 2 hands. In other words, the tuning functions of the cortical patches should evenly span the space of possible actions (Pouget and Sejnowski 1997). This implies that there should be a different activation pattern for each bimanual action and that each pair of actions should be distinguished by the activity of a comparable number of neuronal patches or voxels. Thus, when going from one bimanual action to another, a comparable number of voxels should change their activation. Therefore, we predict that the activity patterns associated with different bimanual actions should be equally dissimilar to each other. To test this, we determined the 9 possible pairwise correlations between patterns that shared the same contralateral finger and submitted these to a 1-factorial repeated-measures ANOVA. The analysis showed that the 9 pairs were roughly equidistant (both $F_{8,48} < 1.35$, $P > 0.24$, for pre- and postcentral ROIs). Thus, the tuning properties of these voxels uniformly spanned the whole space of tested bimanual combinations.

To summarize, we identified a region in the transitional zone between M1 and PM and in the posterior somatosensory cortex that encoded bimanual finger movements in a way that would be maximally useful for the fine control of bimanual actions.

Discussion

During unimanual ipsilateral actions, the BOLD signal in the hand area of the primary motor cortex decreases consistently, indicating reduced synaptic activity (Talelli, Ewas et al. 2008; Talelli, Waddingham et al. 2008). Somewhat more anterior, on the boundary of PM, increases in activity are regularly observed (Rao et al. 1993; Boecker et al. 1994; Kim et al. 1994; Kawashima et al. 1998; Cramer et al. 1999; Hanakawa et al. 2005; Horenstein et al. 2009). The question that has hitherto not been answered is whether these decreases and increases in mean activation during ipsilateral actions indicate finger-specific patterns or just reflect nonspecific tonic signal changes.

Using multivariate analysis, we demonstrate that primary motor and sensory cortices represent ipsilateral finger movements and do so in fundamentally different ways, depending on whether an action is uni- or bimanual. During unimanual actions, we observed strong finger-specific modulation of the ipsilateral sensory motor cortex in an area that overlapped greatly with the area that encoded the contralateral action. More importantly, the ipsilateral finger-specific pattern exactly matched the pattern elicited by finger presses of the equivalent contralateral finger and vanished during bimanual presses. A second representation on the M1/PM boundary and in posterior S1 showed nonlinear encoding of bimanual actions. All results could be clearly observed in each of the individual participants, which led to statistical significance at the group level, despite the relatively low number of participants.

The representation for ipsilateral unimanual movements was strongest in areas that showed a global suppression of the BOLD signal due to the ipsilateral movement, but also extended to regions that were activated during ipsilateral finger presses. Although it is possible that the ipsilateral pattern arises from "less deactivation" in mirror-symmetric circuits, we consider it more likely that 2 separate inter-hemispheric processes are involved in producing this result. The first process automatically "activates" the circuits encoding mirror-symmetric movements of the contralateral hand. Support for the idea that such a mechanism exists comes from the well-known phenomenon of mirror movements during unimanual actions (Duque and Ivry 2009; Sehm et al. 2010; Verstynen and Ivry 2011). However, we show here that the patterns related to the ipsilateral finger movement cannot be solely the sensory consequence of such overt mirror movements. Although we observed some signs of mirror activation in the contralateral hand, the changes were neither strong nor consistent enough to explain the observed activation patterns.

The second process during ipsilateral actions globally "suppresses" activity, most likely to reduce the chance of overt mirror movements. Recent studies have shown that the

suppression of the ipsilateral BOLD signal is correlated with the strength of inter-hemispheric inhibition, as probed by dual-pulse TMS (Talelli, Ewas et al. 2008), making a neural origin of this suppression likely (but see Devor et al. 2008). Specifically, it correlates with inter-hemispheric inhibition at a 40 ms, rather than a 10 ms, interstimulus interval, suggesting the involvement of polysynaptic connections through premotor areas, rather than direct M1-to-M1 inhibition. Unimanual actions are also associated with a suppression of the motor-evoked potential elicited by a TMS pulse to ipsilateral M1 (Duque and Ivry 2009). A recent study showed that this suppression is weakest if the ipsilateral movement is mirror-symmetric to the movement evoked by the TMS pulse (Yedimenko and Perez 2010), a finding consistent with the idea of a superposition of action-specific activation and global suppression. This 2-process model can also account for the fact that the BOLD suppression observed in younger individuals turns into overall activation in older adults (Talelli, Ewas et al. 2008).

During bimanual actions, the strong, mirrored patterns observed during unimanual actions disappeared completely. One possible mechanism explaining this dramatic switch is the gating of inputs through features of the local circuitry (Fries 2009). When the motor cortex is not involved in an action of the contralateral hand, callosal inputs from the other hemispheres can activate the local recurrent network, and the BOLD signal would reflect the ipsilateral action. In contrast, when the local circuitry receives input from a higher-level area to execute a contralateral action, the same presynaptic input may not influence the recurrent activity and the effect on the observed BOLD signal would be minimal. Previous studies have reported that one can decode the direction of ipsilateral arm movements from cortical surface potentials (Ganguly et al. 2009). Our results suggest that this representation should disappear as soon as the motor cortex becomes functionally engaged during a bimanual task.

The mirrored nature of the ipsilateral representation and its disappearance during bimanual movements suggest that it does not play an active role in the control of movement, but rather constitutes a passive overflow of activity that ultimately needs to be suppressed to avoid mirror movements. Whether this mirroring serves other functions, for example, the transfer of motor learning between hemispheres, is an open question that cannot be answered by observational methods such as fMRI alone. It is also possible that the ipsilateral hemisphere plays a more prominent role in the production of complex finger movements. Patients with unilateral motor cortical lesions show no ipsilesional impairment of maximal grip force, but do exhibit some ipsilesional deficits in fine finger control (Noskin et al. 2008). Furthermore, in healthy individuals, skilled sequence production is impaired after repetitive TMS stimulation of the ipsilateral motor cortex (Chen et al. 1997). During such complex movements, a region on the boundary to PM is commonly activated (Catalan et al. 1998; Cramer et al. 1999; Hanakawa et al. 2005; Verstynen et al. 2005; Horenstein et al. 2009; Verstynen and Ivry 2011). For the simple unimanual finger presses studied here, this region only showed weak activation and weak representation of the ipsilateral finger. While the contra- and ipsilateral patterns were also correlated in this region, this correlation was slightly lower than that in other regions. Thus, it is possible that there is an independent ipsilateral finger representation in this region, which would become more clearly visible for more complex actions. The multivariate techniques developed here will allow us to test this hypothesis in future experiments with complex sequential finger movements.

For bimanual actions, we found clear evidence for a second type of ipsilateral finger representation in premotor and parietal cortices. The center of the bimanual representation was located slightly more anterior in the precentral gyrus and more posterior in the postcentral gyrus, relative to the unimanual representation (Donchin et al. 1998).

The localization of the bimanual representation in premotor and parietal cortices appears to contradict the extensive literature that hypothesizes a special role for the SMA in bimanual behaviors (Brinkman 1984; but see Wiesendanger et al. 1994; Kazennikov et al. 1998). We found both ipsilateral and contralateral representations for unimanual finger presses in the SMA (Table 2), but only a rather weak bimanual representation (Fig. 5*A*), which was not significant after correcting for multiple comparisons. One explanation for this lack of finding is that the finger representations in the SMA may be spatially less strongly clustered than those in premotor and parietal cortices. Combined with the restricted spatial resolution of the fMRI, this would lead to poorer classification accuracy.

It needs to be also kept in mind that one of the main arguments for a special role of the SMA in bimanual coordination comes from fMRI studies that reported increased activation for asymmetric bimanual movements compared with the easier symmetric bimanual movements (e.g. Jäncke et al. 2000; Debaere et al. 2001; Ullen et al. 2003). These studies are somewhat problematic as the SMA also shows increased activity during asynergistic compared with easier synergistic "unimanual" hand movements (Ehrsson et al. 2002). Furthermore, single-cell recording studies, in which the tuning properties of cells during bimanual movements were measured, found little evidence for a special role of the SMA. Bimanual tuning was just as strong as in M1 (Donchin et al. 1998, 2001, 2002; Kermadi et al. 1998), the dorsal premotor, and parietal cortex (Kermadi et al. 2000). Our representational fMRI analysis confirms these results, arguing that bimanual movements are encoded not only in the SMA, but also prominently in dorsal premotor and parietal cortices.

The ipsilateral bimanual patterns in these regions were clearly different from the ipsilateral unimanual patterns, as they did not correlate with each other. Rather, the activity of each voxel was determined by a nonlinear function of the contra- and ipsilateral fingers: the response of each voxel to a particular ipsilateral finger heavily depended on the accompanying contralateral finger. Similar nonlinear encoding has been observed on the single neuron level for bimanual arm movements (Donchin et al. 1998). As in our study, the ipsilateral tuning of neurons during bimanual actions showed little relation to the tuning of the same neurons during unimanual actions.

This nonlinear encoding was not related to the difference between symmetric and asymmetric bimanual actions. While we found areas that were more highly activated during asymmetric actions (Fig. 8, green areas), these were spatially separate from areas that encoded individual bimanual finger presses (Fig. 8, blue areas). Instead, the nonlinear encoding of bimanual actions was caused by individual voxels being activated for particular combinations of bimanual finger presses. Such nonlinear basis functions would be useful for learning movement representations, in which commands to

the contralateral hand depend nonlinearly on the context provided by the intended ipsilateral action. Consistent with this proposed function, our analysis shows that the basis functions spanned the space of possible actions evenly—a prerequisite for successful learning (Pouget and Sejnowski 1997).

Recent studies of motor learning indeed suggest that bimanual movements are learned using nonlinear basis functions. For example, the motor system is very slow to adapt to force fields that push the hand either to the left or to the right on a trial-by-trial basis, even if these switches are fully predictable (Wainscott et al. 2005). However, if participants execute bimanual movements, and if each force direction is associated with a unique movement direction of the other hand, such perturbations can be learned much more quickly (Nozaki et al. 2006; Nozaki and Scott 2009; Howard et al. 2010). In the premotor and anterior parietal areas described here, slightly different neuronal populations would be engaged in each bimanual movement combination. Control strategies learned by this population would only weakly generalize to other bimanual combinations, even if these share the same contralateral or ipsilateral movement. Indeed, recent results indicate that the pattern of generalization to other bimanual movement combinations is consistent with this type of nonlinear gain-field encoding of left- and right-hand actions (Yokoi et al. 2011). The ipsilateral encoding found in the bimanual areas would, therefore, not have a direct role in the control of the ipsilateral movement, but rather supply the contralateral controller with the necessary information about the movement state of the other hand, thereby enabling coordinated bimanual actions (Diedrichsen et al. 2010).

Conclusion

Using an information-based definition of representation, we have demonstrated the existence of an anatomically localized representation of ipsilateral actions. Moving beyond nonspecific descriptions of increases and decreases in the BOLD signal, we show that the nature of this ipsilateral cortical representation of movement changes with the behavioral context.

Supplementary Material

Supplementary material can be found at: http://www.cercor.oxfordjournals.org/.

Funding

The work was supported by grants from the National Science Foundation (grant no. BSC 0726685), the Wellcome Trust (grant no. 094874/Z/10/Z), and the James S. McDonnell Foundation, all to J.D., and National Institute of Health (grant no. RO1 NS052804) to J.W.K. The Wellcome Trust Centre for Neuroimaging is supported by core funding from the Wellcome Trust 091593/Z/10/Z. Funding to pay the Open Access publication charges for this article was provided by the Wellcome Trust.

Notes

We thank Richard B. Ivry and Timothy Verstynen for helpful comments on earlier drafts of the paper. *Conflict of Interest*: None declared.

References

Acharya S, Tenore F, Aggarwal V, Etienne-Cummings R, Schieber MH, Thakor NV. 2008. Decoding individuated finger movements using volume-constrained neuronal ensembles in the M1 hand area. IEEE Trans Neural Syst Rehabil Eng. 16:15–23.

Andersson JL, Hutton C, Ashburner J, Turner R, Friston K. 2001. Modeling geometric deformations in EPI time series. NeuroImage. 13:903–919.

Boecker H, Kleinschmidt A, Requardt M, Hanicke W, Merboldt KD, Frahm J. 1994. Functional cooperativity of human cortical motor areas during self-paced simple finger movements. A high-resolution MRI study. Brain. 117(Pt 6):1231–1239.

Brinkman C. 1984. Supplementary motor area of the monkey's cerebral cortex: short- and long-term deficits after unilateral ablation and the effects of subsequent callosal section. J Neurosci. 4:918–929.

Brinkman J, Kuypers HG. 1973. Cerebral control of contralateral and ipsilateral arm, hand and finger movements in the split-brain rhesus monkey. Brain. 96:653–674.

Catalan MJ, Honda M, Weeks RA, Cohen LG, Hallett M. 1998. The functional neuroanatomy of simple and complex sequential finger movements: a PET study. Brain. 121(Pt 2):253–264.

Chen R, Gerloff C, Hallett M, Cohen LG. 1997. Involvement of the ipsilateral motor cortex in finger movements of different complexities. Ann Neurol. 41:247–254.

Chen Y, Namburi P, Elliott LT, Heinzle J, Soon CS, Chee MW, Haynes JD. 2011. Cortical surface-based searchlight decoding. NeuroImage. 56:582–592.

Cramer SC, Finklestein SP, Schaechter JD, Bush G, Rosen BR. 1999. Activation of distinct motor cortex regions during ipsilateral and contralateral finger movements. J Neurophysiol. 81:383–387.

Dale AM, Fischl B, Sereno MI. 1999. Cortical surface-based analysis. I. Segmentation and surface reconstruction. NeuroImage. 9:179–194.

Debaere F, Swinnen SP, Beatse E, Sunaert S, Van Hecke P, Duysens J. 2001. Brain areas involved in interlimb coordination: a distributed network. NeuroImage. 14:947–958.

Devor A, Hillman EM, Tian P, Waeber C, Teng IC, Ruvinskaya L, Shalinsky MH, Zhu H, Haslinger RH, Narayanan SN et al. 2008. Stimulus-induced changes in blood flow and 2-deoxyglucose uptake dissociate in ipsilateral somatosensory cortex. J Neurosci. 28:14347–14357.

Diedrichsen J, Grafton S, Albert N, Hazeltine E, Ivry RB. 2006. Goal-selection and movement-related conflict during bimanual reaching movements. Cereb Cortex. 16:1729–1738.

Diedrichsen J, Ridgway GR, Friston KJ, Wiestler T. 2011. Comparing the similarity and spatial structure of neural representations: a pattern-component model. NeuroImage. 55:1665–1678.

Diedrichsen J, Shadmehr R. 2005. Detecting and adjusting for artifacts in fMRI time series data. NeuroImage. 27:624–634.

Diedrichsen J, Shadmehr R, Ivry RB. 2010. The coordination of movement: optimal feedback control and beyond. Trends Cogn Sci. 14:31–39.

Donchin O, Gribova A, Steinberg O, Bergman H, Cardoso de Oliveira S, Vaadia E. 2001. Local field potentials related to bimanual movements in the primary and supplementary motor cortices. Exp Brain Res. 140:46–55.

Donchin O, Gribova A, Steinberg O, Bergman H, Vaadia E. 1998. Primary motor cortex is involved in bimanual coordination. Nature. 395:274–278.

Donchin O, Gribova A, Steinberg O, Mitz AR, Bergman H, Vaadia E. 2002. Single-unit activity related to bimanual arm movements in the primary and supplementary motor cortices. J Neurophysiol. 88:3498–3517.

Duque J, Ivry RB. 2009. Role of corticospinal suppression during motor preparation. Cereb Cortex. 19:2013–2024.

Ehrsson HH, Kuhtz-Buschbeck JP, Forssberg H. 2002. Brain regions controlling nonsynergistic versus synergistic movement of the digits: a functional magnetic resonance imaging study. J Neurosci. 22:5074–5080.

Fischl B, Rajendran N, Busa E, Augustinack J, Hinds O, Yeo BT, Mohlberg H, Amunts K, Zilles K. 2008. Cortical folding patterns and predicting cytoarchitecture. Cereb Cortex. 18:1973–1980.
Fischl B, Sereno MI, Tootell RB, Dale AM. 1999. High-resolution intersubject averaging and a coordinate system for the cortical surface. Hum Brain Mapp. 8:272–284.
Fries P. 2009. Neuronal gamma-band synchronization as a fundamental process in cortical computation. Annu Rev Neurosci. 32: 209–224.
Friston K, Holmes AP, Ashburner J. 1999. Statistical parameter mapping (SPM).
Ganguly K, Secundo L, Ranade G, Orsborn A, Chang EF, Dimitrov DF, Wallis JD, Barbaro NM, Knight RT, Carmena JM. 2009. Cortical representation of ipsilateral arm movements in monkey and man. J Neurosci. 29:12948–12956.
Hanakawa T, Parikh S, Bruno MK, Hallett M. 2005. Finger and face representations in the ipsilateral precentral motor areas in humans. J Neurophysiol. 93:2950–2958.
Horenstein C, Lowe MJ, Koenig KA, Phillips MD. 2009. Comparison of unilateral and bilateral complex finger tapping-related activation in premotor and primary motor cortex. Hum Brain Mapp. 30: 1397–1412.
Howard IS, Ingram JN, Wolpert DM. 2010. Context-dependent partitioning of motor learning in bimanual movements. J Neurophysiol. 104:2082–2091.
Hutton C, Bork A, Josephs O, Deichmann R, Ashburner J, Turner R. 2002. Image distortion correction in fMRI: a quantitative evaluation. NeuroImage. 16:217–240.
Indovina I, Sanes JN. 2001. On somatotopic representation centers for finger movements in human primary motor cortex and supplementary motor area. NeuroImage. 13:1027–1034.
Jäncke L, Peters M, Himmelbach M, Noesselt T, Shah J, Steinmetz H. 2000. fMRI study of bimanual coordination. Neuropsychologia. 38:164–174.
Kamitani Y, Tong F. 2005. Decoding the visual and subjective contents of the human brain. Nat Neurosci. 8:679–685.
Kamitani Y, Tong F. 2006. Decoding seen and attended motion directions from activity in the human visual cortex. Curr Biol. 16: 1096–1102.
Kawashima R, Matsumura M, Sadato N, Naito E, Waki A, Nakamura S, Matsunami K, Fukuda H, Yonekura Y. 1998. Regional cerebral blood flow changes in human brain related to ipsilateral and contralateral complex hand movements—a PET study. Eur J Neurosci. 10:2254–2260.
Kazennikov O, Hyland B, Wicki U, Perrig S, Rouiller EM, Wiesendanger M. 1998. Effects of lesions in the mesial frontal cortex on bimanual coordination in monkeys. Neuroscience. 85:703–716.
Kermadi I, Liu Y, Rouiller EM. 2000. Do bimanual motor actions involve the dorsal premotor (PMd), cingulate (CMA) and posterior parietal (PPC) cortices? Comparison with primary and supplementary motor cortical areas. Somatosens Mot Res. 17:255–271.
Kermadi I, Liu Y, Tempini A, Calciati E, Rouiller EM. 1998. Neuronal activity in the primate supplementary motor area and the primary motor cortex in relation to spatio-temporal bimanual coordination. Somatosens Mot Res. 15:287–308.
Kim SG, Ashe J, Hendrich K, Ellermann JM, Merkle H, Uagurbil K, Georgopoulos AP. 1993. Functional magnetic resonance imaging of motor cortex: hemispheric asymmetry and handedness. Science. 261:615–617.
Kim SG, Ugurbil K, Strick PL. 1994. Activation of a cerebellar output nucleus during cognitive processing. Science. 265:949–951.
Kriegeskorte N, Goebel R, Bandettini P. 2006. Information-based functional brain mapping. Proc Natl Acad Sci USA. 103:3863–3868.
Kriegeskorte N, Simmons WK, Bellgowan PS, Baker CI. 2009. Circular analysis in systems neuroscience: the dangers of double dipping. Nat Neurosci. 12:535–540.
Maier MA, Armand J, Kirkwood PA, Yang HW, Davis JN, Lemon RN. 2002. Differences in the corticospinal projection from primary motor cortex and supplementary motor area to macaque upper limb motoneurons: an anatomical and electrophysiological study. Cereb Cortex. 12:281–296.
Noskin O, Krakauer JW, Lazar RM, Festa JR, Handy C, O'Brien KA, Marshall RS. 2008. Ipsilateral motor dysfunction from unilateral stroke: implications for the functional neuroanatomy of hemiparesis. J Neurol Neurosurg Psychiatr. 79:401–406.
Nozaki D, Kurtzer I, Scott SH. 2006. Limited transfer of learning between unimanual and bimanual skills within the same limb. Nat Neurosci. 9:1364–1366.
Nozaki D, Scott SH. 2009. Multi-compartment model can explain partial transfer of learning within the same limb between unimanual and bimanual reaching. Exp Brain Res. 194:451–463.
Oldfield RC. 1971. The assessment and analysis of handedness: the Edinburgh inventory. Neuropsychologia. 9:97–113.
Oosterhof NN, Wiestler T, Downing PE, Diedrichsen J. 2011. A comparison of volume-based and surface-based multi-voxel pattern analysis. NeuroImage. 56:593–600.
Pereira F, Mitchell T, Botvinick M. 2009. Machine learning classifiers and fMRI: a tutorial overview. NeuroImage. 45:S199–S209.
Pouget A, Sejnowski T. 1997. Spatial transformations in the parietal cortex using basis functions. J Cogn Neurosci. 9:222–237.
Rao SM, Binder JR, Bandettini PA, Hammeke TA, Yetkin FZ, Jesmanowicz A, Lisk LM, Morris GL, Mueller WM, Estkowski LD *et al.* 1993. Functional magnetic resonance imaging of complex human movements. Neurology. 43:2311–2318.
Rathelot JA, Strick PL. 2009. Subdivisions of primary motor cortex based on cortico-motoneuronal cells. Proc Natl Acad Sci USA. 106:918–923.
Scheperjans F, Hermann K, Eickhoff SB, Amunts K, Schleicher A, Zilles K. 2008. Observer-independent cytoarchitectonic mapping of the human superior parietal cortex. Cereb Cortex. 18:846–867.
Schieber MH. 2002. Motor cortex and the distributed anatomy of finger movements. Adv Exp Med Biol. 508:411–416.
Sehm B, Perez MA, Xu B, Hidler J, Cohen LG. 2010. Functional neuroanatomy of mirroring during a unimanual force generation task. Cereb Cortex. 20:34–45.
Shmuel A, Augath M, Oeltermann A, Logothetis NK. 2006. Negative functional MRI response correlates with decreases in neuronal activity in monkey visual area V1. Nat Neurosci. 9:569–577.
Shmuel A, Yacoub E, Pfeuffer J, Van de Moortele PF, Adriany G, Hu X, Ugurbil K. 2002. Sustained negative BOLD, blood flow and oxygen consumption response and its coupling to the positive response in the human brain. Neuron. 36:1195–1210.
Soteropoulos DS, Edgley SA, Baker SN. 2011. Lack of evidence for direct corticospinal contributions to control of the ipsilateral forelimb in monkey. J Neurosci. 31:11208–11219.
Swisher JD, Gatenby JC, Gore JC, Wolfe BA, Moon CH, Kim SG, Tong F. 2010. Multiscale pattern analysis of orientation-selective activity in the primary visual cortex. J Neurosci. 30:325–330.
Talelli P, Ewas A, Waddingham W, Rothwell JC, Ward NS. 2008. Neural correlates of age-related changes in cortical neurophysiology. NeuroImage. 40:1772–1781.
Talelli P, Waddingham W, Ewas A, Rothwell JC, Ward NS. 2008. The effect of age on task-related modulation of interhemispheric balance. Exp Brain Res. 186:59–66.
Ullen F, Forssberg H, Ehrsson HH. 2003. Neural networks for the coordination of the hands in time. J Neurophysiol. 89:1126–1135.
Verstynen T, Diedrichsen J, Albert N, Aparicio P, Ivry RB. 2005. Ipsilateral motor cortex activity during unimanual hand movements relates to task complexity. J Neurophysiol. 93:1209–1222.
Verstynen T, Ivry RB. 2011. Network dynamics mediating ipsilateral motor cortex activity during unimanual actions. J Cogn Neurosci. 23:2468–2480.
Wainscott SK, Donchin O, Shadmehr R. 2005. Internal models and contextual cues: encoding serial order and direction of movement. J Neurophysiol. 93:786–800.
Wenderoth N, Debaere F, Sunaert S, Swinnen SP. 2005. Spatial interference during bimanual coordination: differential brain networks associated with control of movement amplitude and direction. Hum Brain Mapp. 26:286–300.
Wenderoth N, Debaere F, Sunaert S, van Hecke P, Swinnen SP. 2004. Parieto-premotor areas mediate directional interference during bimanual movements. Cereb Cortex. 14:1153–1163.

Wiesendanger M, Wicki U, Rouiller E. 1994. Are there unifying structures in the brain responsible for interlimb coordination? In: Swinnen SP, Heuer H *et al.*, editors. Interlimb coordination: neural, dynamical, and cognitive constraints. pp. 179–207. San Diego, CA: Academic Press, Inc.

Wiestler T, McGonigle DJ, Diedrichsen J. 2011. Integration of sensory and motor representations of single fingers in the human cerebellum. J Neurophysiol. 105:3042–3053.

Worsley KJ, Marrett S, Neelin P, Vandal AC, Friston KJ, Evans AC. 1996. A unified statistical approach for determining significant voxels in images of cerebral activation. Hum Brain Mapp. 12:900–918.

Yedimenko JA, Perez MA. 2010. The effect of bilateral isometric forces in different directions on motor cortical function in humans. J Neurophysiol. 104:2922–2931.

Yokoi A, Hirashima M, Nozaki D. 2011. Gain field encoding of the kinematics of both arms in the internal model enables flexible bimanual action. J Neurosci. 31:17058–17068.

Yousry TA, Schmid UD, Alkadhi H, Schmidt D, Peraud A, Buettner A, Winkler P. 1997. Localization of the motor hand area to a knob on the precentral gyrus. A new landmark. Brain. 120(Pt 1):141–157.

Zipser D, Andersen RA. 1988. A back-propagation programmed network that simulates response properties of a subset of posterior parietal neurons. Nature. 331:679–684.